Optimization of key parameters towards high performance perovskite solar cells

Elattar A. M.
Department of Chemistry
Faculty of Science, Ain Shams University
Abbassia, Cairo11566, Egypt
amr_elatar@sci.asu.edu.eg

Saber M. R.
Center for Environmental and Smart Technology
Faculty of Science, Fayoum University
Fayoum 63514, Egypt
mrm01@fayoum.edu.eg

Ammar A. M.
Center for Environmental and Smart Technology
Faculty of Science, Fayoum University
Fayoum 63514, Egypt
am4087@fayoum.edu.eg

Khabiri G.
Center for Environmental and Smart Technology
Faculty of Science, Fayoum University
Fayoum 63514, Egypt
gma01@fayoum.edu.eg

Ghannam R.
School of Engineering
Glasgow University
United Kingdom
Rami.Ghannam@glasgow.ac.uk

Khalil M. M. H.
Department of Chemistry
Faculty of Science, Ain Shams University
Abbassia, Cairo11566, Egypt
mostafa_khalil@sci.asu.edu.eg

Khalil A. S. G.
Center for Environmental and Smart Technology
Faculty of Science, Fayoum University
Fayoum 63514, Egypt
asg05@fayoum.edu.eg

***Abstract*— Here, we report important findings regarding underestimated parameters for the synthesis and fabrication of high-performance perovskite solar cells. These parameters include the effect of Fluorine-doped Tin Oxide (FTO) etching, FTO cleaning, the number of compact TiO_2 (c-TiO_2) layer, the number of mesoporous TiO_2 (m-TiO_2) layers and the aging time before Ag deposition. Our results demonstrated that etching of FTO substrate with Zn/ HCl is an essential step and has a major effect on the solar cell's open circuit voltage (Voc), fill factor (FF) and power conversion efficiency (PCE). Furthermore, we demonstrate new and improved protocols for the complete cleaning of FTO substrates. Despite the use of sonication and plasma etching in previous cleaning techniques, SEM images clearly show black clouds in the samples, which may be due to residual Zn particles in the FTO grooves. Thus, a soft toothbrush was used with detergent before sonication to detach the remaining Zn particles. In addition, the optimum number of spin coated layers of compact and mesoporous TiO_2 precursors was investigated. We found that one mesoporous and two compact TiO_2 layers were required to obtain a homogenous pinhole-free compact layer. Consequently, we demonstrate that using these optimized device fabrication procedures, a high efficiency of 17.96% for 6 mol% Co^{3+}-doped TiO_2 solar cells can be obtained in comparison to 16.98% for pristine TiO_2-based cells. Such cells are particularly important for wearable applications that require a small area and a high energy.**

Keywords—Perovskite solar cells, FTO Etching, FTO cleaning, Pinholes-free, Doped-TiO_2

I. INTRODUCTION

Generally, mesoporous perovskite solar cells (PSCs) consist of an n-type semiconducting mesoporous material as an electron transport layer (ETL), followed by a perovskite compound as an absorber layer and a p-type semiconducting material as a hole transport layer (HTL). Miyasaka's group reported the first PSC in 2009, using $CH_3NH_3PbI_3$ ($MAPbI_3$) perovskite as an absorber material with 3.8% power conversion efficiency (PCE) [1]. This PSC architecture has been developed greatly and PCEs reaching 23.3% have been achieved thanks to an optimization of absorber materials, as well as the interface and other thin-film growth developments [2]. Conventional (n-i-p) mesoporous perovskite solar cells, with a configuration of (FTO/TiO_2 compact layer/TiO_2 mesoporous layer (ETL)/ $CH_3NH_3PbI_3$ perovskite/Spiro-OMeTAD (HTL)/ Ag or Au metal contact), have been widely investigated in the literature. However, there is wide range of reported PCEs (11%-18%), which could be attributed to the lack of consistency in the fabrication methods used [3]. Therefore, developing reliable and reproducible fabrication procedure requires further and detailed optimization of the steps. For eample, More *et al.* have studied the effect of FTO substrate cleaning on the efficiency of dye sensitized solar cells (DSSCs) [4]. Heat treatment of FTO substrates after bath sonication was found to enhance the contact of the TiO_2 layer with the FTO substrate, which improves the DSSC PCE from 3.0% to 3.4%. Wu *et al.* also investigated the effect of compact TiO_2 layer thickness on the performance of planar PSCs with a configuration of FTO/compact TiO_2/$CH_3NH_3PbI_3$/Spiro-MeOTAD/Ag [5]. They observed improved performance by increasing c-TiO_2 thickness to 65 nm. Afterwards, PCE decreases due to charge recombination. Liu *et al.* fabricated mesoscopic perovskite solar cell with a configuration of FTO/compact TiO_2/mesoporous TiO_2/$CH_3NH_3PbI_3$/Spiro-MeOTAD/Ag with varied c-TiO_2 thickness [6]. A small thickness of compact TiO_2 was found insufficient to rapidly extract photoelectrons, which decreases short circuit current density, J_{sc}, as well as the PCE. On the other hand, large thickness increased the layer's resistance and resulted in lower transport. Lee *et al*. found that increasing the mesoporous TiO_2 layer thickness resulted in an increase in the interfacial resistance, which in turn decreased the performance of their PSC [7].

Abate *et al.* proposed that the presence of Li-TFSI salt in the spiro-OMeTAD precursor solution scavenges superoxide radicals O_2^- as Li_2O and Li_2O_2 leading to larger proportions of oxidized spiro-$OMeTAD^+$[8]. The oxidation of spiro-OMeTAD is further enhanced by the aging process which enriches this layer with O_2 leading to an increase in the hole mobility and a decrease in the charge recombination. The optimum reported aging time was 24 hours [9]. Higher aging

times (48 hours) led to the formation of PbI_2, which acts as trapping centers that increase recombination rates and therefore decrease the PCE [10].

Doping the TiO_2 layer with various metals such as In, Nb, Fe, Ta and Mg [11], [12] was found to enhance electron transport. Cobalt-doped planar and mesoporous TiO_2 PSCs have been reported to exhibit higher efficiencies (18.0% and 20.0%) in comparison to their pristine counterparts (17.1 and 18.5%) [13].

Herein, some important parameters during the fabrication process have been investigated and optimized, which include the effect of FTO etching, FTO cleaning, the number of c-TiO_2 layers, the number of m-TiO_2 layers, as well as the aging time. Our results demonstrate that high performance PSC can be achieved using etched, pre-cleaned FTO substrates by spin-coating two layers of c-TiO_2 to achieve a homogenous pinhole-free compact layer with 33 aging hours. Furthermore, we have investigated the effect of cobalt doping in the c-TiO_2 layer.

II. Experimental Details

PSCs were fabricated according to the reported method [14] with some modifications. Briefly, FTO glasses were etched with Zn/HCL to get the desired pattern. After that, FTO substrates cleaned with acetone, detergent, distilled water, isopropanol: acetone (1:1) (v: v) and ethanol with sonication for 10 min/each solution.

Preparation of precursor solutions: Pristine TiO_2 compact layer solution: 0.15 M titanium diisopropoxide bis (acetylacetonate) in 1-butanol. For cobalt-doped c-TiO_2, 0.015 g $CoCl_3$ was dissolved in 2 ml 1-butanol and then stirred for 30 min. After that, $CoCl_3$ solution was added to pristine TiO_2 solution to form Co^{3+}-doped TiO_2 solution at different molar ratios (1 mol%, 2 mol%, 4 mol%, 6 mol% and 8 mol%). Finally, spin-coating of doped and un-doped TiO_2 solutions on FTO substrate at 2800 rpm for 20 sec, which were followed by drying at 125 ºC for 5 min. Mesoporous TiO_2 (m-TiO_2) layer was deposited on the c-TiO_2 by spin-coating the TiO_2 colloidal solution containing 121 mg of TiO_2 paste (Dyesol) diluted in 1 mL of 1-butanol solution at 2000 rpm for 20 sec, which was annealed at 500 ºC for 1 h and then UVO was treated for 15 min. PbI_2, CH_3NH_3I, and DMSO (molar ratio 1:1:1) was vortexed in 524 µL of DMF solution at room temperature for 15 min to prepare the perovskite solution. The completely dissolved solution was spin-coated on the m-TiO_2 layer at 4000 rpm for 25 sec and 0.3 ml of diethyl ether was slowly dripped on the rotating substrate in 10 sec before the surface changed to be turbid caused by rapid vaporization of DMF. The dense brown perovskite film was obtained with heating at 65 ºC for 1 min and 100 ºC for 10 min. The 20 µl of spiro-MeOTAD solution, which was consisted of 72.3 mg spiro-MeOTAD, 28.8 µl of 4-tert-butyl pyridine and 17.5 µl of (Li-TFSI) solution (520 mg Li-TSFI in 1 ml acetonitrile) in 1ml of chlorobenzene, was spin-coated on the perovskite layer at 3000 rpm for 30 sec. After that, the fabricated cell was aged inside dark/open place for different aging hours. Finally, Ag electrode was deposited by using thermal evaporator at a constant evaporation rate of 0.10 nm/s.

TABLE 1 PARAMETERS OF CHAMPION $MAPbI_3$ SOLAR CELLS WITH/WITHOUT ETCHING PROCESS; RS: REVERSE SCAN, FS: FORWARD SCAN

Sample	*Voc (V)*	*Jsc (mA/cm²)*	*FF (%)*	*PCE (%)*
Etched PSC, RS	1.02	24.36	67.87	16.86
Etched PSC, FS	1.035	24.00	45.86	11.39
Non-etched PSC, RS	0.285	24.34	62.1	4.3
Non-etched PSC, FS	0.14	20.79	39.45	1.15

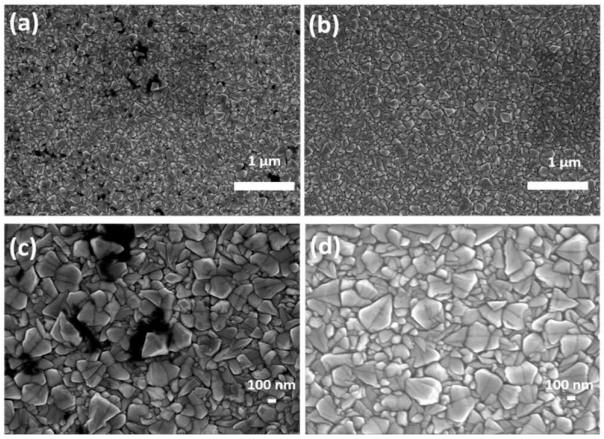

Fig. 1. SEM images of FTO substrate before and after cleaning with (a, c) detergent, (b, d) soft brushes.

III. Results and Discussions

A. FTO Etching Effect

The architecture of the fabricated mesoporous perovskite solar cells is FTO/c-TiO_2/m-TiO_2/ $CH_3NH_3PbI_3$/Spiro-OMeTAD/ Ag. PCEs of the fabricated cells using patterned and un-patterned FTO substrates were compared in order to draw some conclusions on the effect of etching on the cell

TABLE 2 COMPARISON BETWEEN OUR WORK AND LITERATURE WORK WITH THE SAME CELL CONFIGURATION

Ref.	Cell configuration	Maximum PCE%
[3]	FTO/cp-TiO_2/mp-TiO_2/$CH_3NH_3PbI_3$/spiro-OMeTAD/Au	18.01%
[15]	FTO/cp-TiO_2/mp-TiO_2/$CH_3NH_3PbI_3$/spiro-OMeTAD/Au	11.49%
[16]	FTO/cp-TiO_2/mp-TiO_2/$CH_3NH_3PbI_3$/spiro-OMeTAD/Au	13.47%
[17]	FTO/cp-TiO_2/mp-TiO_2/$CH_3NH_3PbI_3$/spiro-OMeTAD/Au	11.64%
[18]	FTO/cp-TiO_2/mp-TiO_2/$CH_3NH_3PbI_3$/spiro-OMeTAD/Au	15.82%
[19]	FTO/cp-TiO_2/mp-TiO_2/$CH_3NH_3PbI_3$/spiro-OMeTAD/Au	15.04%
[20]	FTO/cp-TiO_2/mp-TiO_2/$CH_3NH_3PbI_3$/spiro-OMeTAD/Au	15.51%
[21]	FTO/cp-TiO_2/mp-TiO_2/$CH_3NH_3PbI_3$/spiro-OMeTAD/Au	15.97%
[22]	FTO/cp-TiO_2/mp-TiO_2/$CH_3NH_3PbI_3$/spiro-OMeTAD/Au	11.19%
[23]	FTO/cp-TiO_2/mp-TiO_2/$CH_3NH_3PbI_3$/spiro-OMeTAD/Au	16.30%
Our work	FTO/cp-TiO_2/mp-TiO_2/$CH_3NH_3PbI_3$/spiro-OMeTAD/Ag	18.41%

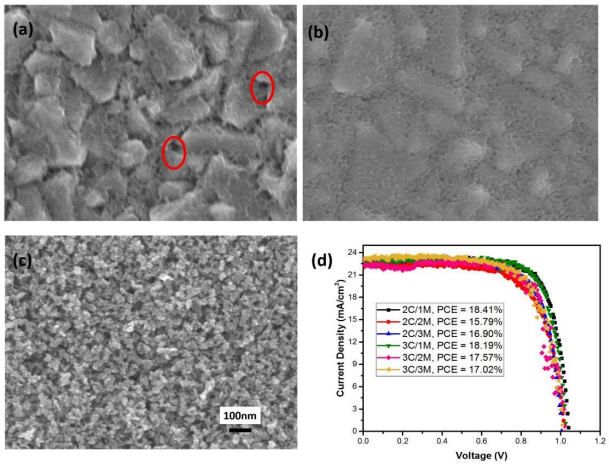

Fig. 2. SEM images of (a) one c-TiO_2 layer, (b) two c-TiO_2 layers (c) 2-layer c-TiO_2/1-layer m-TiO_2. Red circles show pinholes. (d) J–V characteristics of champions of PSCs with different thickness of compact and mesoporous TiO_2 layers, under AM 1.5G one sun illumination (100 mW.cm^{-2}).

performance. The champion etched PSC yield higher performance than that without etching (16.8% and 4.8 % respectively (Table 1). Without etching, deterioration of V_{oc}, FF and PCE values were observed indicating a significant effect of etching on cell performance.

B. FTO Cleaning Effect

SEM images of conventionally cleaned substrates (Fig. 1 a, c) show black clouds attributable to filling FTO grooves with remnant Zn particles from the etching step. Using soft toothbrush during the detergent step, before sonication, proved efficient to detach the remaining Zn particles as shown in Fig.1b, d.

C. Number of TiO_2 Layers Effect

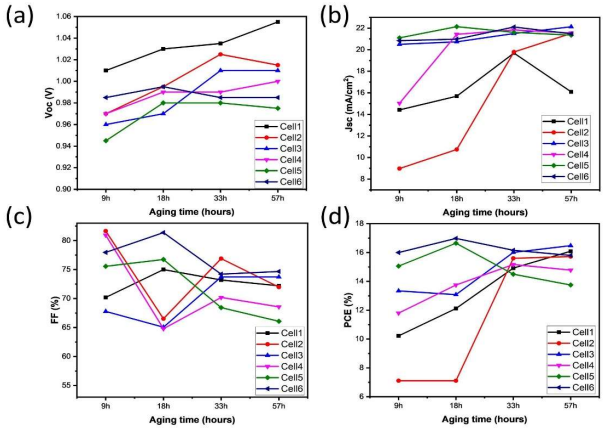

Fig. 3. Photovoltaic parameters Voc, Jsc, FF and PCE, respectively of six different $MAPbI_3$-based PSCs at different aging time in (hours).

The number of c-TiO_2 layers was optimized to obtain a pinhole-free film. The surface morphology of one spin-coated c-TiO_2 layer clearly suffers from pinholes (Fig, 2a) which were efficiently removed up on depositing a second layer (Fig. 2b). The current density versus voltage (J-V) curves shown in Fig. 2d reveal that the configuration of (FTO/2 c-TiO_2/1 m-TiO_2/$MAPbI_3$/spiro/Ag) yield the highest performance (18.41%). Table 2 shows a comparison between our work and previous literature work with cell configuration (FTO/TiO_2/ $MAPbI_3$/Spiro-OMeTAD/Ag or Au).

D. Aging Time Effect

The oxidation of spiro-OMeTAD is a crucial process for enhancing the hole mobility and improving the overall PCEs of the cell. We postulated that the aging of the spiro-OMeTAD layer should enrich this layer with O_2 leading to an increase in the hole mobility and a decrease in the charge recombination due to higher oxidized spiro-OMeTAD$^+$ concentrations. The spiro-OMeTAD deposited devices were kept in a dark, open

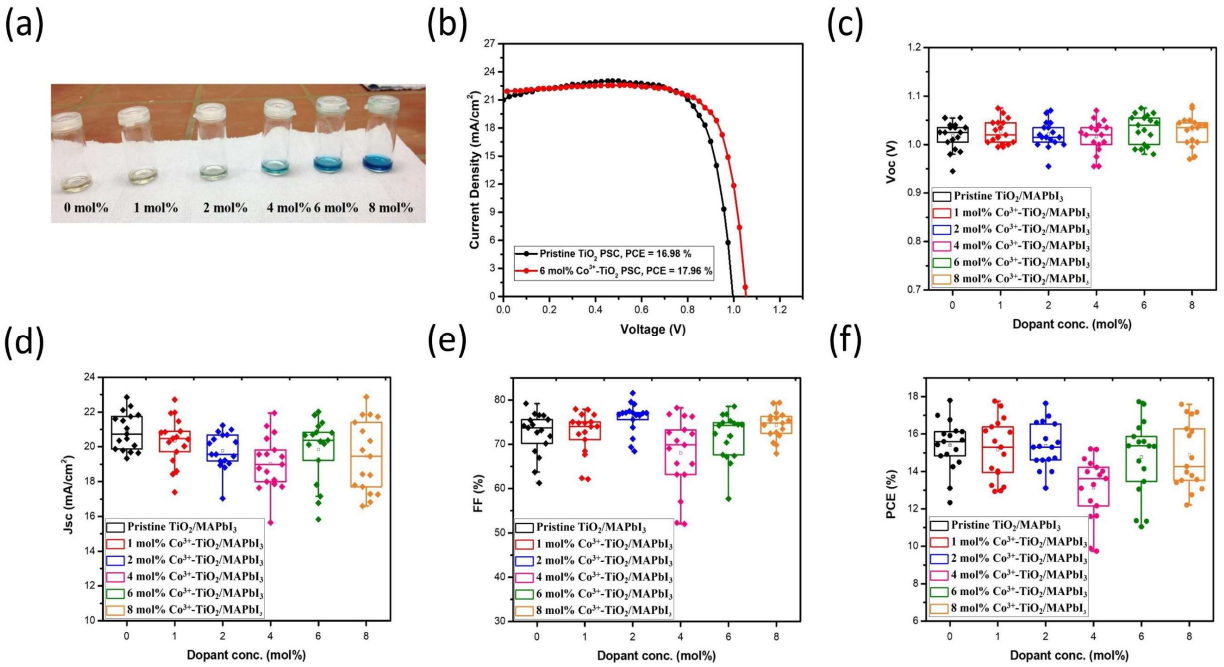

Fig. 4 Solutions of pristine TiO_2 and Co^{3+}-TiO_2 solutions. (b) J–V characteristics of champions of pristine TiO_2 and Co^{3+}-TiO2 PSCs under AM 1.5G one sun illumination (100 mW.cm^{-2}). (c-f) Statistical distribution of the photovoltaic parameters Voc., Jsc., FF. and PCE of the $MAPbI_3$-based PSCs with different Co^{3+}-doping concentrations.

place for different time periods (9, 18, 33 and 57 hours). 150 nm silver contact was then thermally evaporated over aged cells. The overall photovoltaic parameters (J_{sc}, V_{oc} and PCE) were found to increase with aging time till an optimum value of 33h, which could be attributed to significant oxidation of spiro-OMeTAD via O_2 in the atmosphere with the time. After that, steady state was observed during the next 24 hours and this might be due to reaching of saturation state so that no further oxidation was happened. Higher aging times were not accompanied by any enhancement possibly due to potential formation of PbI_2 which acts as trapping centers increasing recombination rates and decreasing PCE [10].

E. Cobalt Doping Effect

Different concentrations (0, 1, 2, 4, 6, and 8 mol%) of cobalt chloride salt were used to prepare cobalt-doped c-TiO_2 precursor solution as discussed in experimental section. Figure 4a exhibits that the color of the Co^{3+}-TiO_2 solution gradually changes to intense blue with the increase of doping concentration. The current density versus voltage (J-V) curves shown in Fig. 4b reveal that the 6 mol% Co-doped device shows higher Voc and Jsc and yields higher performance than that of pristine TiO_2 PSC (17.96% versus 16.98%). The statistics of V_{oc}, J_{sc}, FF and PCE of 117 devices based on different doping conditions (Fig. 4c-f) further supports that 6 mol% Co-doped cells exhibit the highest V_{oc} with mean value 1.04 V while 2 mol% Co-doped cells exhibit the highest FF and PCE with mean values 75.49% and 15.51% respectively. These results exhibit the capability of cobalt to enhance the electron transport properties of TiO_2 layer.

IV. CONCLUSION

We have shown that careful optimization of FTO etching, FTO cleaning, pinhole-free compact TiO_2 layer deposition and aging time are all crucial parameters to obtain reliable and reproducible high performance $MAPbI_3$ PSCs. Best devices were achieved using Zn/HCl etching solutions followed by cleaning using a soft toothbrush with detergent before sonication to detach the remaining Zn particles. The optimum number of layers is two c-TiO_2 and one m-TiO_2 to get homogenous pinhole-free compact layer. Moreover, aging is a crucial step after spiro-OMeTAD layer assembly over (FTO/TiO_2/perovskite) structure. Finally, using Co-doped TiO_2 compact layer (1 mol%, 2 mol%, 4 mol%, 6 mol%, and 8 mol%) has led to higher efficiency (17.96% for 6 mol%) as compared to 16.98% for pristine TiO_2-based cells.

ACKNOWLEDGMENT

This work was partially supported by Egypt's Science, Technology & Innovation Funding Authority (STDF) under grant (34888).

REFERENCES

[1] A. Kojima, K. Teshima, Y. Shirai, and T. Miyasaka, "Organometal Halide Perovskites as Visible-Light Sensitizers for Photovoltaic Cells," *J. Am. Chem. Soc.*, vol. 131, no. 17, pp. 6050–6051, May 2009, doi: 10.1021/ja809598r.

[2] K. T. Cho *et al.*, "Highly efficient perovskite solar cells with a compositionally engineered perovskite/hole transporting material interface," *Energy Environ. Sci.*, vol. 10, no. 2, pp. 621–627, 2017, doi: 10.1039/C6EE03182J.

[3] L. Zhu *et al.*, "Enhancing the efficiency and stability of perovskite solar cells by incorporating CdS and Cd(SCN2H4)2Cl2 into the CH3NH3PbI3 active layer," *J. Mater. Chem. A*, 2019, doi: 10.1039/C8TA09933B.

[4] V. More, V. Shivade, and P. Bhargava, "Effect of Cleaning Process of Substrate on the Efficiency of the DSSC," *Trans. Indian Ceram. Soc.*, vol. 75, no. 1, pp. 59–62, Jan. 2016, doi: 10.1080/0371750X.2016.1149100.

[5] R. Wu *et al.*, "Dependence of device performance on the thickness of compact TiO2 layer in perovskite/TiO2 planar heterojunction solar cells," *J. Renew. Sustain. Energy*, vol. 7, no. 4, p. 43105, Jul. 2015, doi: 10.1063/1.4926578.

[6] H. Liu *et al.*, "Thickness-dependent photovoltaic performance of TiO2 blocking layer for perovskite solar cells," *J. Alloys Compd.*, vol. 736, pp. 87–92, 2018, doi: https://doi.org/10.1016/j.jallcom.2017.11.081.

[7] D. G. Lee *et al.*, "Effect of TiO2 particle size and layer thickness on mesoscopic perovskite solar cells," *Appl. Surf. Sci.*, 2017, doi: https://doi.org/10.1016/j.apsusc.2017.11.124.

[8] A. Abate *et al.*, "Lithium salts as 'redox active' p-type dopants for organic semiconductors and their impact in solid-state dye-sensitized solar cells.," *Phys. Chem. Chem. Phys.*, vol. 15, no. 7, pp. 2572–2579, Feb. 2013, doi: 10.1039/c2cp44397j.

[9] D. Bryant *et al.*, "Light and oxygen induced degradation limits the operational stability of methylammonium lead triiodide perovskite solar cells," *Energy Environ. Sci.*, vol. 9, no. 5, pp. 1655–1660, 2016, doi: 10.1039/C6EE00409A.

[10] G. Liu, X. Xi, R. Chen, L. Chen, and G. Chen, *Oxygen aging time: A dominant step for spiro-OMeTAD in perovskite solar cells*, vol. 10. 2018.

[11] J. Song *et al.*, "Performance enhancement of perovskite solar cells by doping TiO2 blocking layer with group VB elements," *J. Alloys Compd.*, vol. 694, no. C, pp. 1232–1238, 2017, doi: 10.1016/j.jallcom.2016.10.106.

[12] X. Yin, Y. Guo, Z. Xue, P. Xu, M. He, and B. Liu, "Performance enhancement of perovskite-sensitized mesoscopic solar cells using Nb-doped TiO 2 compact," 2015, doi: 10.1007/s12274-015-0711-4.

[13] J. K. Kim *et al.*, "Resolving Hysteresis in Perovskite Solar Cells with Rapid Flame-Processed Cobalt-Doped TiO2," *Adv. Energy Mater.*, vol. 8, no. 29, p. 1801717, Aug. 2018, doi: 10.1002/aenm.201801717.

[14] N. Ahn, D.-Y. Son, I.-H. Jang, S. M. Kang, M. Choi, and N.-G. Park, "Highly Reproducible Perovskite Solar Cells with Average Efficiency of 18.3% and Best Efficiency of 19.7% Fabricated via Lewis Base Adduct of Lead(II) Iodide," *J. Am. Chem. Soc.*, vol. 137, no. 27, pp. 8696–8699, Jul. 2015, doi: 10.1021/jacs.5b04930.

[15] A. I. Rafieh, P. Ekanayake, A. Wakamiya, H. Nakajima, and C. M. Lim, "Enhanced performance of CH3NH3PbI3-based perovskite solar cells by tuning the electrical and structural properties of mesoporous TiO2 layer via Al and Mg doping," *Sol. Energy*, vol. 177, pp. 374–381, 2019, doi: https://doi.org/10.1016/j.solener.2018.11.024.

[16] W. Ke *et al.*, "Perovskite Solar Cell with an Efficient TiO2 Compact Film," *ACS Appl. Mater. Interfaces*, vol. 6, no. 18, pp. 15959–15965, Sep. 2014, doi: 10.1021/am503728d.

[17] T. Su, Y. Yang, G. Dong, T. Ye, Y. Jiang, and R. Fan, "Improved photovoltaic performance of mesoporous perovskite solar cells with hydrogenated TiO2: prolonged photoelectron lifetime and high separation efficiency of photoinduced charge," *RSC Adv.*, vol. 6, no. 69, pp. 65125–65135, 2016, doi: 10.1039/C6RA12205A.

[18] P. Zhang *et al.*, "Performance Enhancement of Mesoporous TiO2-Based Perovskite Solar Cells by SbI3 Interfacial Modification Layer," *ACS Appl. Mater. Interfaces*, vol. 10, no. 35, pp. 29630–29637, Sep. 2018, doi: 10.1021/acsami.8b10062.

[19] N. Aeineh *et al.*, "Optical Optimization of the TiO2 Mesoporous Layer in Perovskite Solar Cells by the Addition of SiO2 Nanoparticles," *ACS Omega*, vol. 3, no. 8, pp. 9798–9804, Aug. 2018, doi: 10.1021/acsomega.8b01119.

[20] B. Parida, A. Singh, M. Oh, M. Jeon, J.-W. Kang, and H. Kim, "Effect of compact TiO2 layer on structural, optical, and performance characteristics of mesoporous perovskite solar cells," *Mater. Today Commun.*, vol. 18, pp. 176–183, 2019, doi: https://doi.org/10.1016/j.mtcomm.2018.12.007.

[21] K. S. Anuratha, H.-S. Peng, Y. Xiao, T.-S. Su, T.-C. Wei, and J.-Y. Lin, "Electrodeposition of nanostructured TiO2 thin film as an efficient bifunctional layer for perovskite solar cells," *Electrochim. Acta*, vol. 295, pp. 662–667, 2019, doi: https://doi.org/10.1016/j.electacta.2018.10.181.

[22] S. F. Shaikh, H.-C. Kwon, W. Yang, R. S. Mane, and J. Moon, "Performance enhancement of mesoporous TiO2-based perovskite solar cells by ZnS ultrathin-interfacial modification layer," *J. Alloys Compd.*, vol. 738, pp. 405–414, 2018, doi: https://doi.org/10.1016/j.jallcom.2017.12.199.

[23] J. Jin *et al.*, "Improving Efficiency and Light Stability of Perovskite Solar Cells by Incorporating YVO4:Eu3+, Bi3+ Nanophosphor into the Mesoporous TiO2 Layer," *ACS Appl. Energy Mater.*, vol. 1, no. 5, pp. 2096–2102, May 2018, doi: 10.1021/acsaem.8b00192.